Bioactive Materials 21 (2023) 241–252

Contents lists available at ScienceDirect

Bioactive Materials

journal homepage: www.keaipublishing.com/en/journals/bioactive-materials

Dendritic cell-mimicking scaffolds for ex vivo T cell expansion

Hye Sung Kim [a,b,1], Tzu-Chieh Ho [a,c,1], Moshe J. Willner [a], Michael W. Becker [c], Hae-Won Kim [b,d,e,f], Kam W. Leong [a,g,*]

[a] Department of Biomedical Engineering, Columbia University, New York, NY, USA
[b] Institute of Tissue Regeneration Engineering, Dankook University, Cheonan, Republic of Korea
[c] Wilmot Cancer Institute, University of Rochester Medical Center, Rochester, NY, USA
[d] Department of Regenerative Dental Medicine, College of Dentistry, Dankook University, Cheonan, Republic of Korea
[e] Department of Nanobiomedical Science and BK21 PLUS NBM Global Research Center for Regenerative Medicine, Dankook University, Cheonan, Republic of Korea
[f] Mechanobiology Dental Medicine Research Center, Dankook University, Cheonan, Republic of Korea
[g] Department of Systems Biology, Columbia University Irving Medical Center, New York, NY, 10032, USA

ARTICLE INFO

Keywords:
Adoptive cell therapy
Ex vivo T cell expansion
Cytotoxic T cell
Dendritic cell membrane
Cell membrane coating
Scaffold

ABSTRACT

We propose an ex vivo T cell expansion system that mimics natural antigen-presenting cells (APCs) for adoptive cell therapy (ACT). Microfiber scaffolds coated with dendritic cell (DC) membrane replicate physicochemical properties of dendritic cells specific for T cell activation such as rapid recognition by T cells, long duration of T cell tethering, and DC-specific co-stimulatory cues. The DC membrane-coated scaffold is first surface-immobilized with T cell stimulatory ligands, anti-CD3 (αCD3) and anti-CD28 (αCD28) antibodies, followed by adsorption of releasable interleukin-2 (IL-2). The scaffolds present both surface and soluble cues to T cells ex vivo in the same way that these cues are presented by natural APCs in vivo. We demonstrate that the DC-mimicking scaffold promotes greater polyclonal expansion of primary human T cells as compared to αCD3/αCD28-functionalized Dynabead. More importantly, major histocompatibility complex molecules derived from the DC membrane of the scaffold allow antigen-specific T cell expansion with target cell-specific killing ability. In addition, most of the expanded T cells (~97%) can be harvested from the scaffold by density gradient centrifugation. Overall, the DC-mimicking scaffold offers a scalable, modular, and customizable platform for rapid expansion of highly functional T cells for ACT.

1. Introduction

Adoptive cell therapy (ACT) with T cells is a powerful tool to treat various diseases such as cancer and infectious disease [1,2]. Ex vivo T cell expansion is a key step in generating clinically effective doses of highly functional T cells for successful ACT [3]. One of the main limitations of personalized ACT is that current clinical approaches require the identification and expansion of T cells through autologous antigen presenting cells such as monocyte-derived dendritic cells (moDCs). Although T cells expanded by moDCs have shown clinical success, moDC-based T cell expansion ex vivo is limited by availability, potential dysfunction, and complex and lengthy culture of autologous moDCs [4–8], resulting in increased duration and cost of T cell products manufacturing.

To overcome these limitations, various artificial antigen presenting cells (aAPCs) have been developed using biomimetic particles- or scaffold-based platforms [9–12]. aAPCs typically provide a T cell receptor (TCR)-mediated activation signal (signal 1), a costimulatory signal (signal 2), and signaling through cytokines (signal 3) [13], mimicking natural APC-T cell interactions. Parameters affecting the outcome of the T cell phenotype and response include the material, size, shape, ligand and ligand density of the scaffold [14]. Especially, the size and shape of aAPCs can have a significant impact on T cell activation by altering the material-cell surface contact area and, in turn, the avidity of TCR–antigen peptide-major histocompatibility complex (pMHC) interactions [15]. For example, micro-sized aAPCs led to greater T cell stimulation by increasing the multi-valent TCR-pMHC interactions as compared with nanosized ones forming only monovalent or divalent

Peer review under responsibility of KeAi Communications Co., Ltd.
* Corresponding author. Department of Biomedical Engineering, Columbia University, New York, NY, USA.
E-mail address: kam.leong@columbia.edu (K.W. Leong).
[1] These authors contributed equally to this work.

https://doi.org/10.1016/j.bioactmat.2022.08.015
Received 26 June 2022; Received in revised form 10 August 2022; Accepted 23 August 2022

interactions with T cells [16,17]. Similarly, rod-shaped nano-/-micro-particles (e.g., carbon nanotubes and mesoporous silica rods) also exhibited increased contact with T cells with multi-avidity interactions due to their large surface area and high aspect ratio, as compared with spherical ones [9,10]. Liposomal or lipid-coated aAPCs provide membrane fluidity when interacting with T cells, increasing stimulatory signal clustering and thus accelerating T cell stimulation [9,11,12]. Interleukin-2 (IL-2) released from a biodegradable PLGA-based aAPCs to stimulate the T cells seeded on the scaffold in a paracrine manner was significantly more potent than just adding the IL-2 to the culture medium [17]. Moreover, the flexible polymeric scaffold facilitated their surface contact with T cells [18,19]. Therefore, there is ample room to improve the aAPC design beyond the minimal requirements of presenting the essential signals.

aAPCs offer scalable and off-the-shelf platforms in a relatively inexpensive, stable and reproducible way. Dynabead, polystyrene microbeads with an iron oxide core, is one of the most commonly used and clinically relevant off-the-shelf systems for polyclonal T cell expansion ex vivo. αCD3/αCD28-functionalized Dynabeads provide two of the essential signals for T cell activation; however, IL-2 has to be exogenously supplemented. This does not mimic how those signals are presented by natural APCs. Moreover, a lack of MHC molecules and sets of co-stimulatory cues (e.g., OX40L, 4-1BB, CD27, CD40L, ICOS, and anti-GITR) in Dynabead limits their use for clinical application in ACT [20–23]. Despite significant advancements in ex vivo T cell expansion systems using aAPCs, several challenges remain such as extremely rare antigen-specific T cell populations, rapid T cell exhaustion, variability among individuals, and costly cytokine supplements for T cell manufacturing.

To address these unmet needs, we developed a scalable, modular, and customizable ex vivo T cell expansion system using dendritic cell-mimicking scaffolds. Micro-sized scaffolds, microfibril, were decorated with dendritic cell membranes to offer increased avidity of TCR-pMHC interactions as compared to conventional platforms with smaller dimensions and fixed stimulatory ligands decoration. Subsequent surface-immobilization of αCD3 and αCD28 on dendritic cell membrane-coated microfibrils allowed polyclonal T cell expansion, while MHC molecules naturally derived from the DC membrane of the scaffold enabled antigen-specific expansion. Material availability, specificity, modularity, and cost-effective features of this platform would not only enable the efficient expansion of highly functional T cells for ACT, but also has the potential for large-scale manufacturing of T cells ex vivo.

2. Results

2.1. Preparation of dendritic cell-mimicking scaffolds

We prepared an ex vivo T cell expansion system based on dendritic cell-mimicking scaffolds (Fig. 1). Here, polymeric microfibril (MF) was used as a scaffold material and was coated with human dendritic cell (DC) membrane. Then, the surface was functionalized with T cell stimulatory ligands, anti-CD3 (αCD3) and anti-CD28 (αCD28) antibodies, and IL-2 was loaded for sustained release of the cytokine to mimic how APCs activate T cells in vivo.

THP-1, a human monocytic leukemia cell line, was differentiated to dendritic cells (Fig. S1) and was fed on 1-Azidoethyl-choline prior to the cell membrane extraction. The concentration of 1-Azidoethyl-choline treated was 0.1 mM where cell viability was >90% (Fig. S2a). As the concentration increased above 0.1 mM, the cell viability decreased, and there was no further increase in the amount of azide groups available for click reaction (Figs. S2b and c). MF was coated with the azide-modified DC membrane (DC@MF) and the αCD3/αCD28 stimuli antibodies functionalized with dibenzocyclooctyne (DBCO) groups were subsequently conjugated to DC@MF via copper-free click reaction (Ab/DC@MF). IL-2 was then loaded to Ab/DC@MF by simple adsorption (IL-2/Ab/DC@MF).

MF was coated with DC membrane by membrane vesicle fusion with MF. By ultrasonication, DC membranes would form vesicles and these vesicles tend to fuse with a solid substrate to reduce their high surface energy [24–26]. MF was coated with varying concentrations of DC membranes ranging from 0.1 mg/mL to 1 mg/mL (Fig. S3). At higher concentrations of DC membrane above 0.1 mg/mL, more unbound cell membrane was observed and was difficult to remove. As MF was coated with Dil-labeled cell membrane (Dil-CM) at a concentration of 0.1 mg/mL, the fluorescence signal from Dil-CM was evenly distributed on microfibrils (Fig. 2a, left). Transmission electron microscopy (TEM) showed a thin membrane layer on the surface of MF (Fig. 2a, right). The surface zeta-potential of DC@MF was similar to that of DC membranes (~-20 mV) (Fig. 2b). Together, these results confirmed the coating of MF with DC membrane.

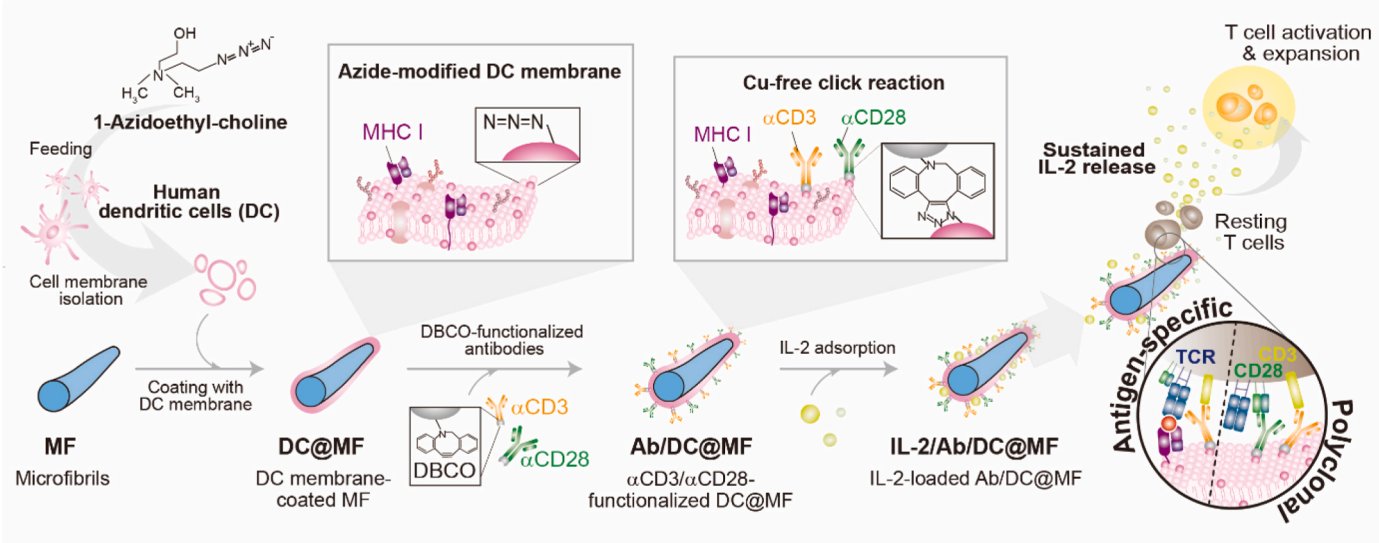

Fig. 1. Schematic of the proposed ex vivo T cell expansion system based on dendritic cell-mimicking scaffolds. To mimic dendritic cells, microfibrils (MF) were coated with dendritic cell membranes, decorated with T cell stimulatory ligands (αCD3 and αCD28), and loaded with IL-2 cytokine. The scaffold allowed polyclonal T cell expansion as well as antigen-specific expansion via MHC molecules naturally derived from the DC membrane of the scaffold. This system mimics how APCs activate T cells in vivo by presenting both surface and soluble cues to T cells ex vivo.

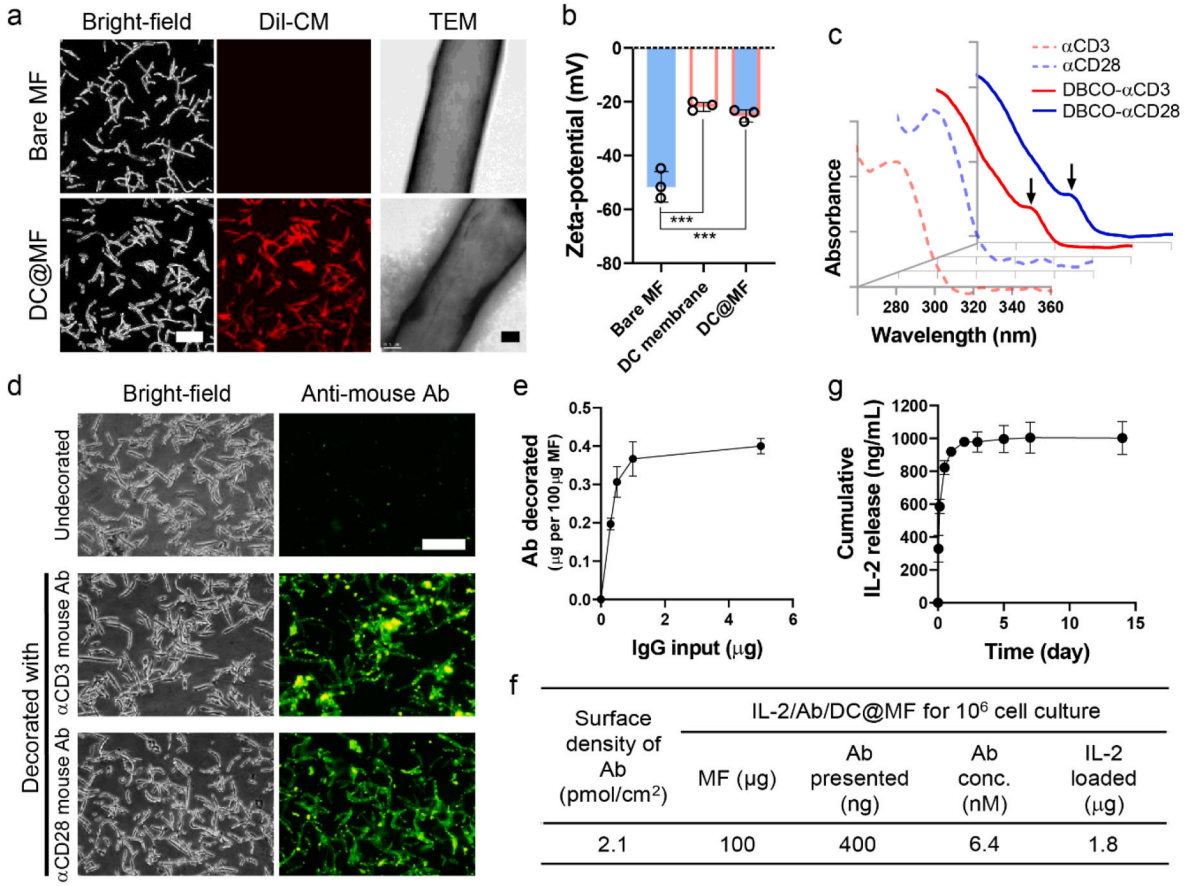

f

Surface density of Ab (pmol/cm^2)	IL-2/Ab/DC@MF for 10^6 cell culture			
	MF (μg)	Ab presented (ng)	Ab conc. (nM)	IL-2 loaded (μg)
2.1	100	400	6.4	1.8

Fig. 2. Characteristics of dendritic cell-mimicking scaffolds. (a) (Left) CLSM images (scale bar, 50 μm) and (right) TEM images (scale bar, 500 nm) of bare MF and DC membrane-coated MF (DC@MF). For CLSM, DC membrane was stained with Dil dye (Dil-CM, red). (b) Zeta-potential of bare MF, DC membrane, and DC@MF (***$p < 0.001$; one-way ANOVA followed by Tukey's post hoc tests). (c) UV–Vis spectra of antibodies functionalized with DBCO groups ($\lambda_{DBCO} = 317$ nm, arrow). (d) Fluorescence microscopy images of DC@MF decorated with αCD3 or αCD28 (scale bar, 100 μm). The αCD3 or αCD28 mouse antibodies decorated on DC@MF were detected and visualized by an anti-mouse secondary antibody labeled with Alexa Flour® 488 (green). (e) Decoration of various inputs of DBCO-functionalized antibodies onto 100 μg DC@MF. (f) Formulations of IL-2/Ab/DC@MF for culture of 10^6 cells. (g) IL-2 release profile of IL-2/Ab/DC@MF.

DC membrane-coated MF was modified with T cell stimulatory ligands, monoclonal mouse anti-human CD3 (αCD3; TCR stimulus) and mouse anti-human CD28 (αCD28; co-stimulatory cue) antibodies. αCD3 and αCD28 were functionalized with DBCO groups and were subsequently conjugated to the azide groups of DC@MF via copper-free click reaction. UV–Vis spectra of DBCO-functionalized αCD3 and αCD28 exhibited a distinguishable peak at 317 nm as compared to the controls (Fig. 2c). The peak at 280 nm was broadened after the DBCO functionalization. It might be due to the random DBCO conjugation of antibodies by the *N*-hydroxysuccinimide reaction. Nevertheless, the binding potential of the Fc and antigen recognition regions of the DBCO-functionalized antibodies click-conjugated constructs can be retained [27]. After the DBCO-functionalized antibodies were conjugated to azide-modified DC@MF, the antibodies decorated on DC@MF were detected and visualized by a fluorescent anti-mouse secondary antibody (Fig. 2d). A fluorescence signal was observed on the surface of the αCD3 or αCD28-decorated DC@MF, suggesting the surface modification of DC@MF with T cell stimulatory ligands. Without azide modification of the cell membranes, a negligible amount of DBCO-functionalized antibodies was adsorbed onto the scaffold, indicating the antibody conjugation to the scaffold was click-chemistry-mediated (Fig. S4). As the amount of azide groups available on the cell membrane layer was consistent, the amount of antibodies decorated on DC@MF was controlled by adjusting the antibody input for the click reaction (Fig. 2e). The maximum amount of antibodies decorated on DC@MF was 0.4 μg/100 μg MF, confirmed by ELISA (Fig. 2f). Subsequently, IL-2 was loaded to the αCD3/αCD28-decorated DC@MF (Ab/DC@MF) by physical adsorption including electrostatic interactions. IL-2 (pI 7.67) is slightly positively charged (+3.77 ± 0.55 mV) while Ab/DC@MF is negatively charged (−24.65 ± 4.40 mV) in neutral pH (Fig. S5a). The maximum IL-2 loading amount of Ab/DC@MF was 1.8 μg/100 μg MF (Fig. S5b). The cumulative IL-2 release profile of IL-2-loaded Ab/DC@MF (IL-2/Ab/DC@MF) exhibited a burst release and reached a plateau within 24 h (Fig. 2g), suggesting a weak and non-specific loading of IL-2 on the membrane. For culturing 10^6 T cells, 100 μg IL-2/Ab/DC@MF was used, presenting 6.4 nM stimuli at a surface density of 2.1 pmol/cm^2 and a loading of 1.8 μg IL-2 (Fig. 2f).

2.2. *Dendritic cell-mimicking scaffolds induce robust T cell activation*

Primary human T cells ($CD3^+$) were isolated from peripheral blood (Fig. S6) and were cultured with bare MF, DC@MF, or Ab/DC@MF, and the T cell-microfibril interaction was monitored by live cell imaging. Cell movement trajectories showed that T cells rapidly recognized the DC membrane-coated surface and tethered to DC@MF and Ab/DC@MF. In contrast, bare MF would not be able to arrest the T cells at the initial stage of cell seeding (Fig. 3a). At 1.5 h of cell culture, most T cells ended up tethering to Ab/DC@MF, some cells remained adhered to DC@MF, and only a few cells adhered to bare MF (Fig. 3b). Cells adhered to DC@MF or bare MF only for a few minutes, soon detaching and migrating again. Therefore, the distance traveled by T cells cultured with Ab/DC@MF was significantly shorter (Fig. 3c), and the cell

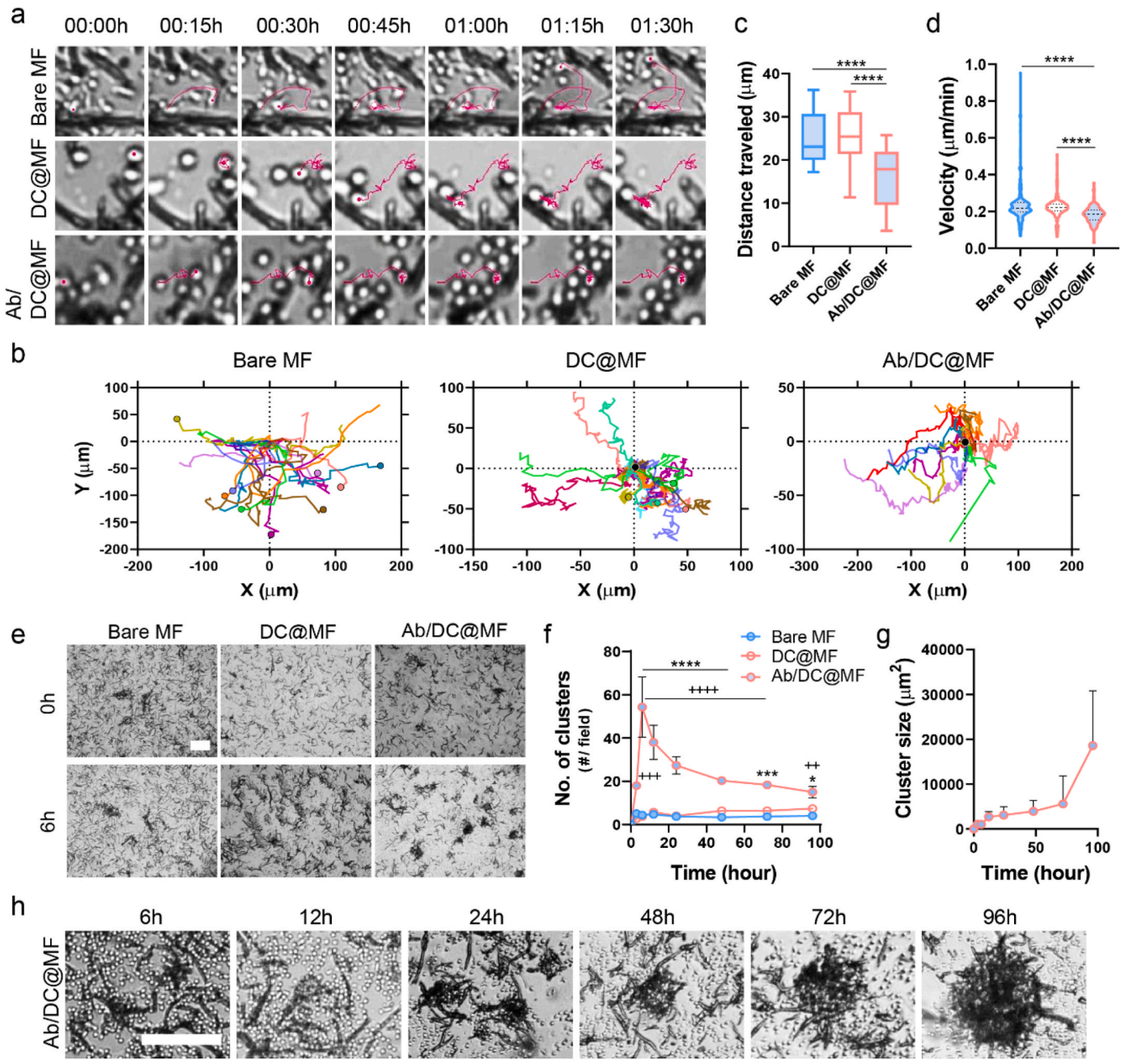

Fig. 3. Ab/DC@MF presenting T cell stimulatory ligands induce robust T cell tethering and activation. (a–d) Cell movement analysis for 1.5 h of initial T cell seeding with bare MF, DC@MF, or Ab/DC@MF. (a) Representative cell movement tracking (pink). (b) T cell tracks (9 cells, 3 cells/field, 3 image fields) plotted with respect to the MF position (0,0). Cells at the end position are marked with circle. More cells ended up binding onto Ab/DC@MF as compared to the other MF groups. (c) T cell track lengths and (d) velocity (25 cells/field, 3 image fields, $^{****}p < 0.0001$; one-way ANOVA followed by Tukey's post hoc tests). (e) Bright-field microscopy images showing initial T cell clustering with Ab/DC@MF within 6 h (scale bar, 100 μm). (f) The number of T cell clusters with bare MF, DC@MF, or Ab/DC@MF ($^{*}p < 0.05$, $^{***}p < 0.001$, and $^{****}p < 0.0001$ versus DC@MF; $^{++}p < 0.01$, $^{+++}p < 0.0001$, and $^{++++}p < 0.0001$ versus Bare MF; two-way ANOVA followed by Tukey's post hoc tests), (g) T cell cluster size of Ab/DC@MF, and (h) representative bright-field microscopy images of T cell clusters with Ab/DC@MF for 96 h of culture (scale bar, 100 μm).

movement velocity of T cells cultured with Ab/DC@MF also increased as compared to that of bare MF and DC@MF (Fig. 3d). These results indicate that the ligands on the decorated MF were efficient in capturing T cells.

Unlike bare MF and DC@MF, T cells activated by Ab/DC@MF formed clusters within 6 h of cell culture (Fig. 3e) and proliferated as clusters for 72 h (Movie S1). Time-lapse videos of the T cell culture with Ab/DC@MF exhibited that single cells were tethered to the microfibril within 3 h of cell culture, and cell-microfibril clusters began to fuse with other cells and clusters within 12 h (Movie S2). Small clusters gradually fused and became bigger over time. The number of clusters in the Ab/DC@MF group rapidly increased until 6 h of culture and decreased after that due to cluster fusion (Fig. 3f). The cluster size gradually increased over time (Fig. 3g and h). The MF scaffold was not internalized by T cells (Fig. S7). Given that T cell clustering is considered an initial onset of T cell activation and proliferation [28], these results suggest that Ab/DC@MF triggers a robust T cell activation by presenting T cell stimulatory ligands.

Supplementary data related to this article can be found at https://doi.org/10.1016/j.bioactmat.2022.08.015.

2.3. Dendritic cell-mimicking scaffolds are superior to Dynabead for polyclonal expansion of primary human T cells

Primary human T cells were cultured with αCD3/αCD28-functionalized Dynabead or various microfibril formulations (bare MF, DC@MF, Ab/DC@MF, and IL-2/Ab/DC@MF) (Table 1). Various final stimuli concentrations of Ab/DC@MF ranging from 1.0 nM to 12.8 nM were tested for T cell activation (Fig. S8). The final concentration of stimuli was proportional to the additional amount of scaffolds. The minimal concentration of stimuli showing robust T cell clustering was 6.4 nM. At a higher concentration of stimuli, the number of T cell clusters formed for 3 days was similar, but there was a larger number of free scaffolds not interacting with T cells. Eventually, for culturing 10^6 T cells, 100 μg of IL-2/Ab/DC@MF presenting 6.4 nM stimuli and 1.8 μg IL-2 were used (Fig. 2f and Table 1). Dynabead at a cell-to-bead ratio of 1:1 presented 1393.9 nM stimuli which is a 218-fold higher concentration than the microfibrils. All groups were cultured in T cell media supplemented with IL-2 (30 U/mL) except for the IL-2/Ab/DC@MF* group.

Both Dynabead and Ab/DC@MF activated T cells by stimulating TCR and co-stimulatory molecules (Fig. 4a). Therefore, progressively large T cell clusters were observed in both groups on day 3 of culture, and once those clusters gradually dissociated, cells continued to proliferate as single cells for 7 days of culture (Fig. 4b). Bare MF and DC@MF did not induce any T cell activation and expansion due to a lack of T cell stimulatory ligands. Dynabead exhibited a smaller cluster size and a larger number of clusters as compared to Ab/DC@MF (Fig. 4c).

T cells cultured with IL-2-loaded Ab/DC@MF (IL-2/Ab/DC@MF) generated a larger number of clusters with bigger sizes than those cultured with Ab/DC@MF without IL-2 loading. Fold expansion profiles showed that T cells rapidly proliferated within 7 days of culture with Dynabead, Ab/DC@MF, or IL-2/Ab/DC@MF (Fig. 4d). On day 14 of culture, Ab/DC@MF yielded a 2-fold greater T cell expansion than Dynabead (Fig. 4e). Fold expansion of T cells cultured with IL-2/Ab/DC@MF was further improved to 7-fold and 4-fold as compared to Dynabead and Ab/DC@MF, respectively. Although Dynabead presented a 218-fold higher concentration of stimuli than Ab/DC@MF, Ab/DC@MF was superior for T cell expansion. Moreover, as Dynabead (a cell-to-bead ratio of 1:0.05) presented a similar concentration of stimuli (6.9 nM) as Ab/DC@MF did (6.4 nM), the T cell expansion rate of Ab/DC@MF was still 10-fold greater than that of Dynabead (Fig. S9). These results indicate the potency of the dendritic cell-mimicking scaffolds in polyclonal T cell expansion.

All Ab/DC@MF groups promoted substantial CD8-biased skewing while Dynabead promoted a more balanced $CD4^+$ and $CD8^+$ T cell expansion (Fig. 4f and S10a). In addition to promoting a nearly 2-7-fold greater expansion than Dynabead at day 14 of culture, the Ab/DC@MF groups yielded few T cells co-expressed with the exhaustion markers PD-1 and LAG-3 (<5%) with high viability (>72%), similar to the Dynabead (Fig. 4g, S10b, and S11). The cytotoxic functions of expanded T cells (i.e., targeting and killing ability) were further evaluated with antigen-specific activation and expansion.

To better understand the effect of IL-2 loading onto Ab/DC@MF, T cells were expanded with IL-2/Ab/DC@MF in the absence of IL-2 supplement in the media for 14 days (IL-2/Ab/DC@MF*). Notably, the fold expansion, rate of expansion, CD8-to-CD4 ratio, and % $PD\text{-}1^+LAG\text{-}3^+$ were similar to those of the group supplemented with IL-2 in the media. These results suggest that the IL-2 release of Ab/DC@MF would significantly improve polyclonal T cell expansion by closely mimicking the APC behavior. We also confirmed that this ex vivo T cell expansion system supported reproducible polyclonal T cell expansion (Fig. S12).

Expanded T cells were harvested from microfibrils by density gradient centrifugation (Fig. 4h). The T cell/microfibril mixture was layered using Ficoll®, a density gradient medium, and centrifuged. Cell fraction was located in the intermediate layer, and microfibril fraction settled at the bottom layer of the gradient. The cell harvesting efficiency of ~97% was determined by counting cell numbers before and after the separation. Furthermore, flow cytometry analysis showed that the microfibril fraction was discarded after the separation (Fig. 4i). Together, these results suggest that the T cells can be readily harvested from the microfibrils after expansion.

2.4. Dendritic cell-mimicking scaffolds enable antigen-specific T cell expansion

We next assessed whether the dendritic cell-mimicking scaffold could be used for antigen-specific expansion of rare human T-cell subpopulations. Here, cytomegalovirus (CMV) was selected as a target model. IL-2/αCD28/DC@MF was used for antigen-specific T cell expansion. To prepare CMV-specific scaffolds, microfibril was coated with the membrane of monocyte-derived dendritic cells (moDC) obtained from a patient with CMV ($HLA\text{-}A2^+$ donor) (Fig. S13). αCD28 was subsequently conjugated, and IL-2 was loaded to the moDC membrane-coated microfibril (IL-2/αCD28/DC@MF). CMV-specific antigen peptides could be loaded to MHC I originating from DC membranes of the scaffold, presenting antigens to T cells via TCR-pMHC interactions. αCD28 of the scaffold would co-stimulate CD28 of T cells during T cell activation (Fig. 5a). Fluorescence microscopy images of IL-2/αCD28/DC@MF stained with Alexa Fluor 594-labeled anti-mouse IgG antibody and FITC-labeled anti-human HLA-A2 antibody showed the co-localization of αCD28 and MHC I on the surface of the scaffold (Fig. 5b and S14). CMV-specific T cells were also obtained from the same patient and expanded ex vivo with either autologous moDC or IL-2/αCD28/DC@MF presenting antigen peptides (IV9 from HIV-1 RT epitope and CEF20 from CMV pp65, respectively). IV9 was used as a non-specific antigen peptide. CMV-specific T cells formed clusters and drastically expanded with moDC or IL-2/αCD28/DC@MF presenting CEF20 (Fig. 5c and S15). The CEF20-presenting scaffold formed larger clusters and yielded greater fold expansion than moDC pulsed with CEF20 (Fig. 5d and e). The expanded T cell functions were evaluated by co-culturing with T2 target cells presenting CEF20. As T2-to-T cell ratios increased, the viability of T2 target cells decreased in all groups (Fig. 5f). In addition, T cells expanded with the CEF20-presenting scaffold and exhibited greater killing of target cells. At a ratio of T2-to-T cell at 25, T cells expanded with either CEF20-presenting moDC or IL-2/αCD28/DC@MF strongly responded to T2 cells presenting their cognate

Table 1
Formulations of Dynabead and IL-2/Ab/DC@MF for polyclonal T cell expansion.

For 10^6 cell culture	Cell-to-bead ratio	Additional amount	Antibody presented			IL-2 loaded (nM)	IL-2 supplemented in media (nM)
			Total amount (μg)	Surface density (pmol/cm^2)	Conc. (nM)		
Dynabead[a]	1:0.05	5000 ea	0.4	868	6.9	–	1.3
	1:1	10^6 ea	82.8		1393.9	–	
IL-2/Ab[b]/DC@MF	–	100 μg	0.4	2.1	6.4	58	

[a] Dynabeads functionalized with αCD3 and αCD28.
[b] 1:2 M ratio of αCD3:αCD28 for decoration.

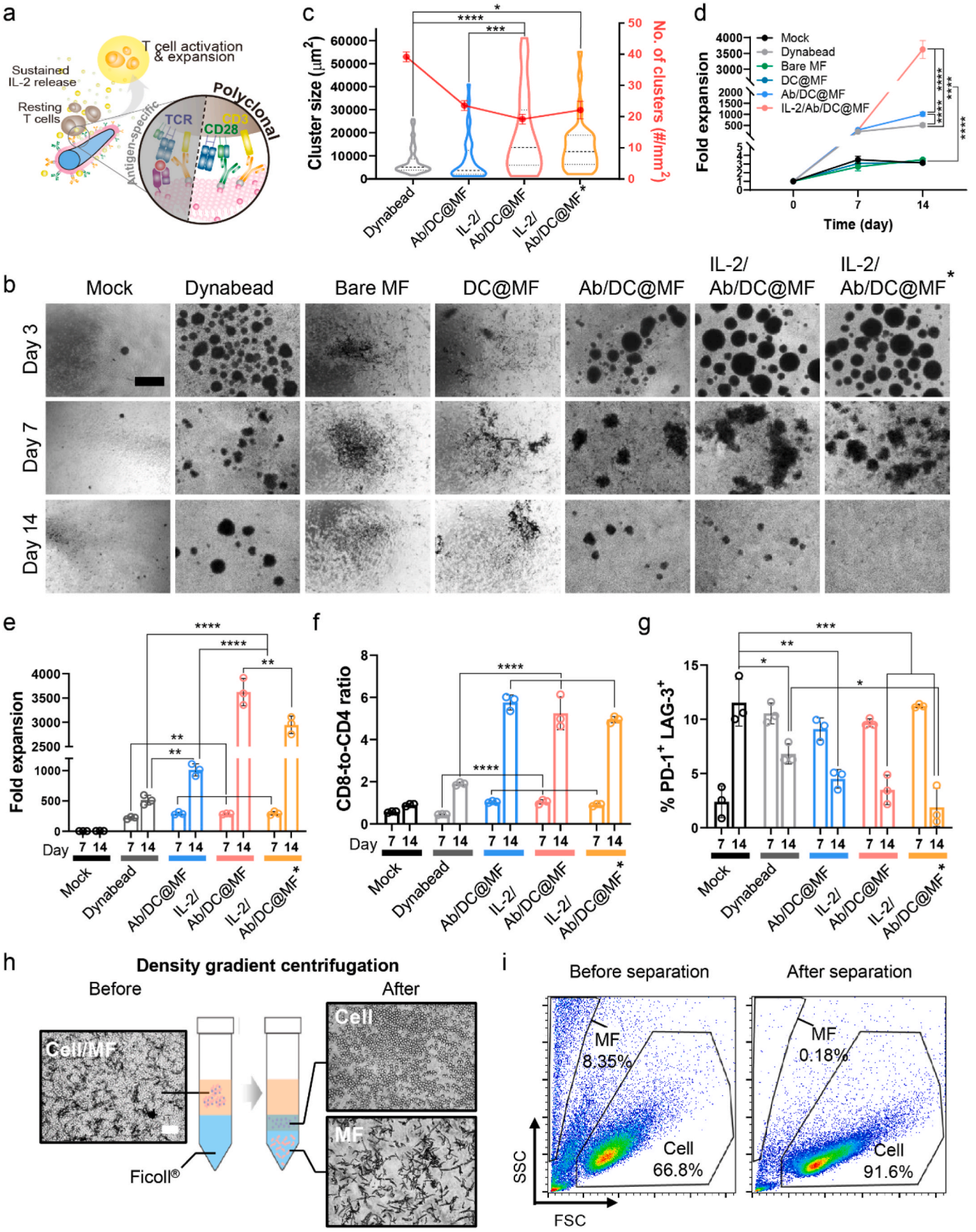

(caption on next page)

Fig. 4. Polyclonal expansion of primary human T cells. (a) Schematic of polyclonal T cell expansion stimulated by IL-2/Ab/DC@MF. (b) Representative bright-field microscopy images of primary human T cells cultured with Dynabead (a cell-to-bead ratio of 1:1), bare MF, DC@MF, Ab/DC@MF or IL-2/Ab/DC@MF (scale bar, 100 μm). *indicates T cell culture without additional IL-2 supplements in culture media. (c) T cell cluster size and the number of T cell clusters on day 3 of expansion. (d–g) T cell expansion using Dynabead, bare MF, DC@MF, Ab/DC@MF, or IL-2/Ab/DC@MF for 14 days. (d) Expansion profiles. (e) Fold expansion at day 7 and day 14. (f) CD8-to-CD4 ratio and (g) co-expression of PD-1 and LAG-3 among $CD3^+$ cells expanded by Dynabead or MFs. (h) T cell isolation process using a density gradient centrifugation method (scale bar, 100 μm). T cells were separated from MFs due to the density difference. (i) Scatter profiles for expanded T cells with MFs before and after separation. SCC, side scatter; FSC, forward scatter. Data in (c–g) represent mean ± s.d of n = 3 and are representative of at least two independent experiments. $^*p < 0.05$, $^{**}p < 0.01$, $^{***}p < 0.001$, and $^{****}p < 0.0001$; two-way ANOVA followed by Tukey's post hoc tests.

antigens, as indicated by IFN-γ and TNF-α co-expression and in vitro killing of target cells (Fig. 5g–i). Together, these results demonstrate the ability of dendritic cell-mimicking scaffolds to expand highly functional T cells in an antigen-specific manner.

3. Discussion

We demonstrate that dendritic cell-mimicking scaffolds can activate T cells ex vivo by presenting both surface and soluble cues to T cells, akin to what endogenous APC would do in vivo. Three essential signals are required for efficient T cell activation; (i) TCR activation by antigen recognition, (ii) co-stimulation, and (iii) cytokine-mediated activation and expansion [13]. The DC-mimicking scaffold coated with DC membrane and modified with T cell stimulatory ligands, αCD3 and αCD28, could activate TCRs by bypassing antigen recognition via MHC-antigen complexes and instead directly stimulate downstream signaling of TCR co-receptor CD3. Thus, αCD3-induced T cell activation is non-specific and polyclonal, leading to activation of all T cells regardless of the subset. αCD28, a co-stimulatory signal, would enhance T cell response to the TCR stimulation. Furthermore, our scaffold presents various co-stimulatory membrane-bound proteins derived from the DC membrane, including CD14, CD80, CD83, CD86, and CD209, which can potentially be involved in TCR clustering. In addition, MHC molecules naturally derived from the DC membrane enable the scaffold to expand T cells in an antigen-specific manner. The DC membrane layer of the scaffold also served as an IL-2 cytokine reservoir. The scaffold can thus provide the third essential signal of IL-2 for T cell activation, mimicking the directional cytokine secretion of natural APCs in vivo. Therefore, the dendritic cell-mimicking scaffold not only significantly increased polyclonal and antigen-specific cell expansion, but also promoted more substantial CD8-biased skewing than widely used T cell expansion systems (i.e., Dynabead and moDC). This indicates that the current system is suitable for manufacturing cytotoxic T lymphocytes products (e.g., CAR-T) that are capable of rapid and efficient killing of endogenous antigen expressing cells (i.e., cancer cells and virus-infected cells).

The stimulatory ligand surface density and ligand mobility are important determinants for T cell activation. Differences in particle or scaffold dimensions have implications due to the TCR cluster size-dependent T cell activation [29–31]. For example, larger particles can have multivalent binding with TCR-pMHC clusters. Particles with larger size (300–600 nm in diameter) formed larger TCR clusters and achieved a longer duration of attachment via increased avidity as compared to smaller ones (50 nm in diameter), leading to more efficient T cell activation [29]. We believe that the micro-sized scaffold, 3.4 ± 1.6 μm in diameter and 55.5 ± 23.8 μm in length, is beneficial to induce large stimulatory ligand clustering as compared to particle-based T cell expansion systems. Interestingly, although the surface density of T cell stimulatory ligands on the scaffold (2.1 pmol/cm^2) was 413-fold lower than that on Dynabead (868 pmol/cm^2), the T cell fold-expansion of the scaffold was 2-fold greater than that of Dynabead on day 14 of culture. We speculate the cell membrane fluidity of the scaffold might have contributed to this effect since natural APCs dynamically rearrange and cluster receptors on their surface for enhanced TCR clustering with T cells [32,33]. Lipid-based artificial APCs (aAPCs) have been developed to mimic the fluidic characteristic of natural DC membrane [9,11,12]. The surface fluidity allows T cell ligands freely diffuse within the lipid bilayer. When the scaffold encounters T cells, the lateral diffusion of the membranes promotes the formation of receptor pre-clustering for T cell recognition and also relocates the T cell ligands in response to binding TCRs, leading to efficient signal transduction [34–36]. Such a spatial organization is restricted if the membrane was fixed [37]. This can be difficult to achieve with Dynabead where the stimulatory ligands are covalently fixed and presented at a constant surface density.

Bulky microfibrils with a high aspect ratio (3.4 ± 1.6 μm in diameter and 55.5 ± 23.8 μm in length) generated larger T cell clusters as compared to Dynabead (4.5 μm in diameter), implying more T cells could interact with individual microfibril than with the smaller Dynabead. Furthermore, microfibril fractions form interfibrous macropores in the T cell clusters, reducing the compaction of the cluster and increasing oxygen/nutrient transportation [38], resulting in more viable cells at the core of the clusters with microfibrils than with Dynabeads. Moreover, the larger the scaffold is, the easier it can be removed from the expanded cells.

Further, we exploited the high surface-to-volume ratio of the microfibril scaffold to present T cell stimulatory ligands as well as to deliver IL-2. Cytokines can be loaded to cell membrane-coated scaffolds by physical adsorption such as van der Waals interactions, hydrogen bonding, hydrophobic interactions, and electrostatic interactions [26,39–41]. The DC membrane layer of the scaffold thus served as a reservoir for IL-2, and the scaffold showed a burst release within 24 h by simple diffusion due to the weak and non-specific binding of IL-2 to the cell membrane layer. In vivo, directional cytokine secretion from APC to T cells occurs during antigen presentation [42,43]. Previous works demonstrated that sustained delivery of IL-2 from artificial APCs significantly improved $CD8^+$ T cell activation as compared to delivering IL-2 in the media as a soluble bolus [9,17,44]. Likewise, the scaffold releasing IL-2 in a sustained manner enhanced T cell expansion even without additional IL-2 supplementation in the media for 2 weeks, indicating that the IL-2-releasing scaffold potentiates the effect of IL-2 by mimicking paracrine signaling of natural APCs. Additionally, IL-2/Ab/DC@MF showed even lower exhaustion levels (~3%) than Ab/DC@MF (~5%) and Dynabeads (~7%) at day 14 (Fig. 4g). Several studies reported that material-based aAPC systems have minimal exhaustions [9,45], but the underlying mechanism has not been elucidated yet. We assume this may be due to the sustained delivery of IL-2 by IL-2/Ab/DC@MF, unlike Ab/DC@MF and Dynabead [46,47].

The dendritic cell-mimicking scaffolds offer an economical platform for large-scale production of T cells ex vivo, as a prolonged culture with complex cytokine cocktails can be costly. Unlike live cells, this synthetic scaffold-based system can be stored for extended periods. Large-scale manufacturing of the scaffold is readily achievable since electrospinning is an industrial process. As compared to the traditional ex vivo T cell expansion system based on autologous moDCs, the current system not only saves manufacturing time but also requires a relatively small number of moDCs. For example, 1 million moDCs are commonly required for activating 1.5 million T cells but cell membranes isolated from 1 million moDCs can prepare 1.2 mg scaffolds which can in turn activate 12 million T cells. Furthermore, this system has excellent ex vivo T cell activation efficiency with low doses of T cell stimulatory ligands and IL-2 cytokine.

Noteworthy, this system is a modular platform that can present diverse cues specific to target cells or diseases. For example, electrospun fiber-based scaffolds can be tailored to tune their size, dimension, composition and configuration [48–50]. The cell membrane can be

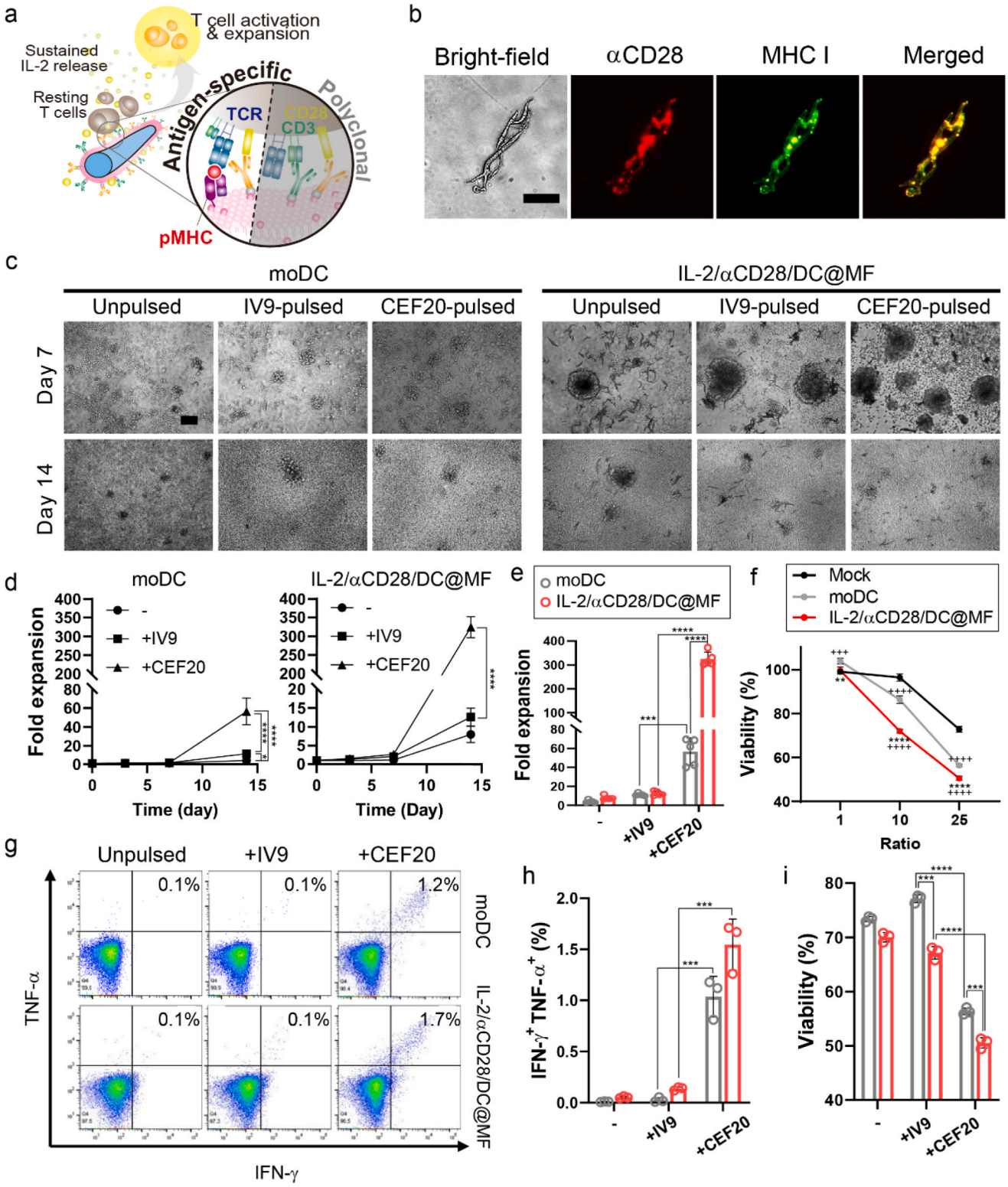

Fig. 5. Antigen-specific expansion of primary human T cells. (a) Schematic of antigen-specific T cell expansion stimulated by IL-2/αCD28/DC@MF. (b) Fluorescence microscopy images of IL-2/αCD28/DC@MF stained with an anti-mouse IgG antibody (red) and an anti-human HLA-A2 antibody (green) (scale bar, 50 μm) for detecting αCD28 and MHC I, respectively. (c) Bright-field microscopy images of CMV-specific T cells cultured with autologous monocyte-derived DC (moDC) or IL-2/αCD28/DC@MF (scale bar, 100 μm). Prior to culture, moDC were pulsed with IV9 or CEF20 (HIV or CMV antigen peptides, respectively) and IL-2/αCD28/DC@MF was loaded with those antigen peptides. (d) T cell expansion profiles of the moDC and IL-2/αCD28/DC@MF groups. -, unpulsed; +IV9, pulsed/loaded with HIV antigen peptides; +CEF20, pulsed/loaded with CMV antigen peptides. (e) Fold expansion at day 14 of CMV-specific T cell culture. (f–i) In vitro T cell functional studies. CMV-specific T cells expanded for 14 days were co-cultured with T2 cells pulsed with CEF20. (f) Viability of T2 target cells at varying T2-to-T cell ratios. (g, h) Flow cytometric analysis showing IFN-γ and TNF-α cytokine production of T cells co-cultured with T2 cells at a ratio of 25. (i) T2 cell viability at a ratio of 25 after 4 h of co-culture. Data in (d–i) represent mean ± s.d of n = 3 and are representative of at least two independent experiments. *$p < 0.05$, **$p < 0.01$, ***$p < 0.001$, and ****$p < 0.0001$; two-way ANOVA followed by Tukey's post hoc tests.

engineered to tune affinity, specificity, surface cue partitioning, or release kinetics of cytokine payloads [51,52]. Since the scaffold is injectable, this system can be further applied to other fields, possibly including in vivo T cell activation and prophylactic vaccination.

The current system requires optimization of the cell harvesting step. Although the scaffold could be separated from the expanded T cells by density gradient centrifugation, incomplete scaffold removal may cause manufacturing failure of the T cell products. Our future studies will be focused on developing a fibrous mesh-based ex vivo T cell manufacturing system that is more practical for large-scale cell production and free from the cell harvest issue.

4. Conclusion

We developed dendritic cell-mimicking scaffolds by coating microfibril with dendritic cell membranes, followed by decoration of T cell-stimulatory ligands and IL-2. Our dendritic cell-mimicking scaffold induced polyclonal T cell expansion by stimulating CD3 and CD28 of T cells and providing proliferative cytokine IL-2 in a paracrine manner. Moreover, MHC I molecules derived from the DC membrane of the scaffold allowed antigen-specific T cell activation and expansion with target cell-specific killing ability. In addition, cells were readily harvested from the scaffold by density gradient centrifugation. The current work suggests a design that not only promotes ex vivo T cell expansion, but also offers a large-scale manufacturing platform with ease of use, modularity, and material availability.

5. Materials and methods

5.1. THP-1 cell differentiation into dendritic cells

The THP-1 human monocytic leukemia cell line (TIB-202) was obtained from the American Type Culture Collection (ATCC). THP-1 cells were cultured in RPMI 1640 (Gibco) supplemented with 10% fetal bovine serum (FBS, Gibco), 1% penicillin-streptomycin (P/S, Gibco) and 0.05 mM 2-mercaptoethanol (Gibco), and the cells were maintained in a humidified incubator with 5% CO_2 at 37 °C. For THP-1 cell differentiation into dendritic cells, THP-1 cells were seeded at a density of 5×10^5 cells/mL in a T-75 flask and treated with phorbol 12-myristate 13-acetate (PMA, 10 ng/mL, Sigma). After 24 h of treatment, human IL-4 (1000 IU/mL, Prosepc) was added to the media and incubated for another 72 h. Dendritic cell-specific surface markers on THP-1-derived dendritic cells were examined by flow cytometry.

5.2. Preparation of azide-modified DC membrane

THP-1-derived dendritic cells were fed on 0.1 mM 1-Azidoethylcholine (JBC-CLK-065, Jena Bioscience) in complete medium for 24 h. The azide-modified cells were harvested and resuspended in a hypotonic lysis buffer (20 mM Tris-HCl (pH 7.5), 10 mM KCl, 2 mM $MgCl_2$, and 1X protease inhibitor cocktail (Sigma-Aldrich) and incubated for 15 min at 4 °C. The lysate was mechanically fragmented with an ultrasonic cell disruptor (QSonica Sonicators) and then centrifuged at 3200×*g* for 5 min to remove cell debris. The supernatant was collected and centrifuged at 10,000×*g* for 30min at 4 °C. The pelleted cell membrane was resuspended in PBS supplemented with 1X protease inhibitors and the mixture was ultrasonicated. The cell membrane was quantified by measuring the UV absorbance of proteins at 280 nm (NanoDrop™ 2000, Thermo Fisher Scientific). For labeling cell membranes, cells were stained with Vybrant™ Dil Cell-Labeling Solution (5 μL for 10^6 cells/mL, Thermo Fisher Scientific) for 10 min at 37 °C prior to cell membrane extraction.

The purified DBCO-functionalized antibodies were analyzed by UV–Vis spectrophotometry (NanoDrop™ 2000, Thermo Fisher Scientific).

5.3. Fabrication of microfibril

Microfibril was fabricated by fragmenting electrospun PCL microfibers as described previously [38,53]. Briefly, PCL (MW 50 kDa, Polysciences, Inc.) was dissolved in a chloroform/methanol mixture (3:1, v/v) at a concentration of 20% (w/v). The PCL solution was electrospun at 15 kV at a flow rate of 1 ml/h through a 27 G needle. Electrospun PCL microfibers were deposited in an ethanol batch at a batch-to-needle distance of 20 cm. Electrospun microfibers were fragmented using a grinder and then were hydrolyzed in 1 M sodium hydroxide at 37 °C for 3 h. Microfiber fragments were collected by centrifugation at 12,000 rpm for 10 min, were thoroughly washed with distilled water, and lyophilized.

5.4. Preparation of IL-2/Ab/DC@MF

5.4.1. Coating microfibril with azide-modified DC membrane

Azide-modified DC membrane (0.1 mg protein) was ultrasonicated for 5min and then mixed with microfibrils (1 mg) in PBS (1 mL, pH 7.4). The mixture was incubated at room temperature for 30 min and then further incubated at 4 °C for 12 h with vigorous shaking at 200 rpm. DC membrane-coated microfibril (DC@MF) was collected by centrifugation at 8000 rpm for 5 min and was washed with PBS to remove the unbound cell membrane. DC@MF was observed by transmission electron microscopy (TEM, Talos F200X, Thermo Fisher Scientific). TEM samples were stained with phosphotungstic acid (2%, w/v) for 1 min prior to observation. Dil-labeled cell membrane (Dil-CM) was used for fluorescence microscopy (Eclipse TS100, Nikon). Zeta-potential of microfibrils were measured by dynamic light scattering analysis with a Zetasizer (Nano ZS90, Malvern Panalytical).

5.4.2. DBCO functionalization of activating antibodies

DBCO-PEG_4-NHS (A134-10, ClickChemistryTools, USA) was added to monoclonal mouse anti-human CD3 (αCD3, 317302, Biolegned) or monoclonal mouse anti-human CD28 (αCD28, 302902, BioLegend) antibody (DBCO-PEG_4-NHS:antibody = 50:1 M ratio) and incubated at 4 °C overnight. DBCO-functionalized antibodies were purified using a centrifugal filter device (Amicon Ultra-0.5, NMWL 10 kDa, Millipore) at 7000 rpm at 4 °C for 30 min. The purified DBCO-functionalized antibodies were analyzed by UV–Vis spectrophotometry (NanoDrop™ 2000, Thermo Fisher Scientific).

5.4.3. Copper-free click reaction for conjugating DBCO-functionalized antibodies to DC@MF

For click reaction, DBCO-functionalized antibodies were mixed with azide-modified DC@MF (100 μg) at a final concentration of 20 μg/mL and 40 μg/mL for αCD3 and αCD28, respectively, in PBS (pH 7.4) and incubated for 3 h at 37 °C. After washing, the fluorescent secondary antibody Alexa Fluor 488-conjugated goat anti-mouse IgG (A-11001, Invitrogen) was added to verify the conjugation. The samples were observed under a fluorescence microscope (Eclipse TS100, Nikon). The amount of conjugated antibodies was quantified by enzyme-linked immunosorbent assay (ELISA, E55-104, BETHYL Lab., Inc).

5.4.4. IL-2 loading and release of antibodies-conjugated DC@MF (Ab/DC@MF)

Recombinant human IL-2 (2 μg, 589102, BioLegend) was added to αCD3 and αCD28-conjugated DC@MF (Ab/DC@MF, 100 μg) in PBS (0.1 mL, pH 7.4) and incubated for 1 h at room temperature with shaking. The amount of IL-2 loaded onto Ab/DC@MF was evaluated by measuring the amount of unbound IL-2 in the supernatant after the loading by ELISA (ELH-IL2-5, Raybiotech). For release study, IL-2 loaded Ab/DC@MF (IL-2/Ab/DC@MF, 100 μg) was incubated in a release buffer (PBS (pH 7.4) containing 1% (w/v) BSA, 1 mL) for 14 days. The supernatant (0.1 mL) was collected and supplemented with fresh release buffer (0.1 mL) at each time point. The amount of IL-2

released was quantified by ELISA.

5.5. Primary human T cell isolation

Human peripheral blood was obtained from the Center for Advanced Laboratory Medicine at Columbia University (IRB-AAAQ5750). PBMCs were enriched from human peripheral blood in a Ficoll (17144002, Cytiva) gradient, then isolated using a pan T cell isolation kit (130-096-535, Miltenyi Biotec) to obtain $CD3^+$ T cells for polyclonal T cell expansion study. The donor information is described in Table S1. T cells were cultured in advanced RPMI 1640 medium supplemented with 10% FBS, 2 mM L-glutamine (Gibco), 1% P/S, and recombinant human IL-2 (30 U/mL, BioLegend).

5.6. Polyclonal T cell expansion

Isolated human T cells were mixed with αCD3/αCD28 Dynabead (11161D, Gibco) or microfibrils (bare MF, DC@MF, Ab/DC@MF and IL-2/Ab/DC@MF) and cultured for up to 2 weeks. T cells (1×10^6 cells/mL) were stimulated with Dynabead (a cell-to-bead ratio of 1:0.05 or 1:1) or microfibrils (100 μg). Media was changed every 2–3 days, and fresh media was added to maintain the cell suspension at a density of $0.5\text{-}1x10^6$ cells/mL. All groups were cultured in T cell media supplemented with IL-2 (30 U/mL) except for the IL-2/Ab/DC@MF* group. Cell fold expansion was evaluated by counting live cells with a hemocytometer using Trypan blue exclusion. Fold expansion was calculated by dividing the number of cells at the respective time point by the number of cells seeded at the start of culture.

5.7. Cell tracking analysis

T cells were seeded with microfibrils and imaged every 30 s for 96 h with a cell movie analyzer (JuLI™ Br, NanoEntek). T cells were tracked using a series of phase-contrast images with Image J plugin MTrackJ, and trajectories were plotted with respect to the microfibril. T cell migration velocity was calculated by dividing the distance traveled by each time frame. The number and size of T cell and microfibril clusters were analyzed by Image J.

5.8. T cell separation by density gradient centrifugation

After 3 days of T cell expansion using microfibrils, the cells and microfibrils were dissociated by pipetting and spun down at 1000 rpm for 5 min. The cell pellet was resuspended in RPMI 1640 containing 10% FBS (2 mL) and mixed with HBSS (2 mL, Gibco) (cell suspension: HBSS = 1:1 (v/v)). The mixture was carefully transferred to a tube containing Ficoll (3 mL) and spun down at 400×*g* for 30 min. The top layer of a Ficoll gradient was discarded, and the intermediate layer was collected and washed with HBSS (10 mL) and spun down again at 1000 rpm for 5 min. Cell number was counted with a hemocytometer using Trypan blue exclusion. Flow cytometry measurements were performed gating on cells and microfibril subsets in SSC vs. FSC plots before and after separation.

5.9. Antigen-specific expansion of primary human T cells

5.9.1. T cells and monocyte isolation from a CMV-infected patient

For antigen-specific T cell expansion study, fresh human peripheral blood Leukopak from a patient with cytomegalovirus (CMV) was purchased from StemExpress (LE001F). PBMCs were enriched from Leukopak in a Ficoll gradient. Human CMV-specific monocytes were isolated from PBMCs using CD14 MicroBeads (130-050-201, Miltenyi Biotec). The donor information is described in Table S1.

5.9.2. CMV-specific monocyte differentiation into DCs and pulsation with antigen peptides

Human CMV-specific monocytes ($CD14^+$ cells) were seeded at a concentration of 1×10^6 cells/mL in RPMI 1640/AIM V (1:1 (v/v), Gibco) medium containing 6% human serum AB (100512, GemCell), 1% P/S, Gentamicin (0.01 mg/mL, Gibco), human IL-4 (1000 IU/mL, CYT-211, ProSpec) and human GM-CSF (1000 IU/mL, CYT-221, ProSpec). For differentiating monocytes into dendritic cells, on day 3 of culture, LPS (500 IU/mL, Sigma) was added to culture plates. Monocyte-derived dendritic cells (moDCs) were harvested after being cultured for 2 more days and their immunophenotype was analyzed by flow cytometry analysis.

5.9.3. Preparation of microfibrils for CMV-specific T cell expansion

CMV-specific moDC were fed on azide-choline and their membrane was extracted as described above. Microfibrils were coated with the azide-modified moDC membrane and DBCO-functionalized αCD28 (40 μg/mL in PBS (pH 7.4)) was conjugated via copper-free click reaction. αCD28-decorated moDC@MF (αCD28/DC@MF) was stained with antibodies against Alexa Fluor 594-conjugated goat anti-mouse IgG (A-11001, Invitrogen) and FITC-labeled mouse anti-human HLA-A2 (343303, BioLegend) for detecting αCD28 and MHC I, respectively, and visualized co-localization of those stimuli on the microfibril.

5.9.4. CMV-specific T cell expansion using moDC or IL-2/αCD28/DC@MF

Prior to T cell expansion, moDC were seeded at a density of 2×10^5 cells/cm^2 and pulsed with 10 μg/mL antigen peptides (CEF20, cytomegalovirus, CMV pp65 (495–503), AS-28328 or IV9 (476–484), HIV-1 RT Epitope, AS-61524, AnaSpec) for 12 h. CMV-specific T cells (3×10^5 cells/cm^2) were added to moDC unpulsed or pulsed with the antigen peptides (moDC:T cell = 1:1.5) and were cultured in the presence of IL-2 (200 IU/mL) for 2 weeks.

αCD28/DC@MF was used for antigen-specific T cell expansion. The antigen peptides (either CEF20 or IV9, 20 μg) were incubated with αCD28/DC@MF (100 μg) in PBS (0.1 mL) overnight at 37 °C. After loading, microfibrils were washed with PBS to remove unloaded antigen peptides. IL-2 (2 μg) was loaded to antigen-loaded αCD28/DC@MF (100 μg) in PBS (0.1 mL) for 1 h prior to the culture. CMV-specific T cells (1×10^6 cells/mL) were mixed with IL-2/αCD28/DC@MF (100 μg) loaded with CMV- or HIV-antigen peptides and were cultured for 2 weeks. Media was supplemented with IL-2 and was changed every 2–3 days.

5.9.5. In vitro killing assay

The T2 (174 x CEM.T2) human lymphoblast cell line was obtained from ATCC and was cultured in Iscove's Modified Dulbecco's Medium (IMDM, Gibco) supplemented with 10% FBS and 1% P/S. T2 cells were stained with 20 μM Calcein AM for 30 min at 37 °C. T2 cells were either unpulsed or pulsed with 10 μg/mL CEF20 in serum-free IMDM for 2 h at 37 °C. Subsequently, expanded T cells (1×10^5 cells) were cultured with T2 cells at varying ratios (T2: T = 1:1, 1:10, and 1:25) in phenol red free medium containing 5% (v/v) human serum. After 4 h of co-culture, cells were spun down and pelleted, and the fluorescence intensity of the supernatant was measured by a plate reader (λ_{ex} = 490 nm and λ_{em} = 590 nm, FLUOstar OPTIMA, BMG Labtech).

5.9.6. Cytokine production assay

T2 cells were either unpulsed or pulsed with 10 μg/mL CEF20 for 2 h at 37 °C. Subsequently, expanded T cells (1×10^5 cells) were cultured with T2 cells at a ratio of 25. After 1 h of co-culture, Brefeldin A (00450651, Invitrogen) was added to inhibit cytokine secretion, and then cultured for another 4 h. Cells were stained and evaluated for IFN-γ and TNF-α by flow cytometry.

5.9.7. Flow cytometry analysis

For immunophenotype analysis of DCs, THP-1-derived dendritic cells or monocyte-derived dendritic cells were washed with 1X PBS with 0.5%

(v/v) PBS and were stained with antibodies against human (FITC, clone HCD14, BioLegend) CD80 (PerCP-eFluor 710, clone 2D10.4, eBioscience), CD83 (APC, clone HB15e, eBioscience), CD86 (PE, clone IT2.2, eBioscience) and CD209 (PE-Cy7, clone eB-h209, eBioscience) for 30 min at 4 °C. For T-cell population analysis, cells were stained with CD3/CD4/CD8a Antibody Cocktail (eBioscience) or antibodies against human LAG-3 (CD223, Alexa Fluor 647, clone 11C3C65, BioLegend) and PD-1 (CD279, Brilliant Violet 421, clone EH12.2H7, BioLegend). After antibody staining, cells were washed and incubated with 4′, 6 diamidino-2-phenylindole (DAPI) (Invitrogen) or 7AAD (BD Pharmingen) for staining live/dead cells. For detecting the intracellular cytokine production, cells were first stained with antibodies against human surface marker CD3/CD4/CD8 (eBioscience) and live/dead reagent DAPI at 4 °C in dark. Cells were washed and fixed/permeabilized using Fixation Buffer (BioLegend) and Intracellular Staining Permeabilization Wash Buffer (BioLegend) according to the manufacturer's protocol. Then, fixed/permeabilized cells were resuspended in Intracellular Staining Permeabilization Wash Buffer and incubated with antibodies against human intracellular cytokine TNF-α (PE-Cy7, clone MAb11, BioLegend) and IFN-γ (PE/Dazzle 594, clone B27, BioLegend). All flow cytometry analyses were performed using LSRFortessa or LSR II (BD Biosciences) and results were analyzed using FlowJo software (BD).

5.10. Statistical analysis

All values were expressed as mean ± standard deviation unless otherwise indicated. Statistical evaluations of data were performed using Student's *t*-test, one-way or two-way ANOVA followed by Tukey's post hoc tests (GraphPad Prism). In all cases, $p < 0.05$ was considered statistically significant.

Ethics approval and consent to participate

Human peripheral blood was obtained from the Center for Advanced Laboratory Medicine at Columbia University (IRB-AAAQ5750).

CRediT authorship contribution statement

Hye Sung Kim: Conceptualization, Methodology, Validation, Investigation, Writing – original draft, Writing – review & editing, Visualization, Funding acquisition. **Tzu-Chieh Ho:** Methodology, Validation, Investigation, Writing – original draft, Writing – review & editing, Visualization. **Moshe J. Willner:** Investigation, Writing – review & editing. **Michael W. Becker:** Writing – review & editing. **Hae-Won Kim:** Writing – review & editing, Funding acquisition. **Kam W. Leong:** Supervision, Writing – review & editing, Funding acquisition.

Declaration of competing interest

The authors declare that they have no conflicts of interest.

Acknowledgments

The authors would like to thank Dr. Pawel Muranski and Dr. Edoardo Migliori (Columbia University Herbert Irving comprehensive cancer center) for scientific discussions and suggestions. This research was supported by the School of Engineering and Applied Science of Columbia University and the National Research Foundation of Korea (2020R1F1A1072699, 2018K1A4A3A01064257, and 2021R1A5A2022318) and Dankook University (Priority Institute Support Program in 2021, Global Research Program).

Appendix A. Supplementary data

Supplementary data to this article can be found online at https://doi.org/10.1016/j.bioactmat.2022.08.015.

References

[1] N.P. Restifo, M.E. Dudley, S.A. Rosenberg, Adoptive immunotherapy for cancer: harnessing the T cell response, Nat. Rev. Immunol. 12 (4) (2012) 269–281.
[2] S.A. Rosenberg, N.P. Restifo, J.C. Yang, R.A. Morgan, M.E. Dudley, Adoptive cell transfer: a clinical path to effective cancer immunotherapy, Nat. Rev. Cancer 8 (4) (2008) 299–308.
[3] C. Yee, G. Lizee, A.J. Schueneman, Endogenous T-cell therapy: clinical experience, Cancer J. 21 (6) (2015) 492–500.
[4] C.A. Klebanoff, L. Gattinoni, D.C. Palmer, P. Muranski, Y. Ji, C.S. Hinrichs, Z. A. Borman, S.P. Kerkar, C.D. Scott, S.E. Finkelstein, S.A. Rosenberg, N.P. Restifo, Determinants of successful CD8(+) T-cell adoptive immunotherapy for large established tumors in mice, Clin. Cancer Res. 17 (16) (2011) 5343–5352.
[5] F.T. Wen, R.A. Thisted, D.A. Rowley, H. Schreiber, A systematic analysis of experimental immunotherapies on tumors differing in size and duration of growth, OncoImmunology 1 (2) (2012) 172–178.
[6] M. Wolfl, P.D. Greenberg, Antigen-specific activation and cytokine-facilitated expansion of naive, human CD8(+) T cells, Nat. Protoc. 9 (4) (2014) 950–966.
[7] F. Veglia, D.I. Gabrilovich, Dendritic cells in cancer: the role revisited, Curr. Opin. Immunol. 45 (2017) 43–51.
[8] S. Satthaporn, A. Robins, W. Vassanasiri, M. El-Sheemy, J.A. Jibril, D. Clark, D. Valerio, O. Eremin, Dendritic cells are dysfunctional in patients with operable breast cancer, Cancer Immunol. Immunother. 53 (6) (2004) 510–518.
[9] A.S. Cheung, D.K.Y. Zhang, S.T. Koshy, D.J. Mooney, Scaffolds that mimic antigen-presenting cells enable ex vivo expansion of primary T cells, Nat. Biotechnol. 36 (2) (2018). -+.
[10] T.R. Fadel, F.A. Sharp, N. Vudattu, R. Ragheb, J. Garyu, D. Kim, E. Hong, N. Li, G. L. Haller, L.D. Pfefferle, S. Justesen, K.C. Herold, T.M. Fahmy, A carbon nanotube-polymer composite for T-cell therapy, Nat. Nanotechnol. 9 (8) (2014) 639–647.
[11] Q. Ding, J. Chen, X.H. Wei, W.Q. Sun, J.H. Mai, Y.Z. Yang, Y.H. Xu, RAFTsomes containing epitope-MHC-II complexes mediated CD4+T cell activation and antigen-specific immune responses, Pharm Res-Dordr 30 (1) (2013) 60–69.
[12] P.F. Zhang, Y.X. Chen, Y. Zeng, C.G. Shen, R. Li, Z.D. Guo, S.W. Li, Q.B. Zheng, C. C. Chu, Z.T. Wang, Z.Z. Zheng, R. Tian, S.X. Ge, X.Z. Zhang, N.S. Xia, G. Liu, X. Y. Chen, Virus-mimetic nanovesicles as a versatile antigen-delivery system, P Natl Acad Sci USA 112 (45) (2015) E6129–E6138.
[13] J.B. Huppa, M.M. Davis, T-cell-antigen recognition and the immunological synapse, Nat. Rev. Immunol. 3 (12) (2003) 973–983.
[14] A. Isser, N.K. Livingston, J.P. Schneck, Biomaterials to enhance antigen-specific T cell expansion for cancer immunotherapy, Biomaterials 268 (2021).
[15] J.W. Hickey, A.Y. Isser, F.P. Vicente, S.B. Warner, H.Q. Mao, J.P. Schneck, Efficient magnetic enrichment of antigen-specific T cells by engineering particle properties, Biomaterials 187 (2018) 105–116.
[16] M.F. Mescher, Surface contact requirements for activation of cytotoxic T lymphocytes, J. Immunol. 149 (7) (1992) 2402–2405.
[17] E.R. Steenblock, T.M. Fahmy, A comprehensive platform for ex vivo T-cell expansion based on biodegradable polymeric artificial antigen-presenting cells, Mol. Ther. 16 (4) (2008) 765–772.
[18] J.C. Sunshine, K. Perica, J.P. Schneck, J.J. Green, Particle shape dependence of CD8+T cell activation by artificial antigen presenting cells, Biomaterials 35 (1) (2014) 269–277.
[19] R.A. Meyer, J.C. Sunshine, K. Perica, A.K. Kosmides, K. Aje, J.P. Schneck, J. J. Green, Biodegradable nanoellipsoidal artificial antigen presenting cells for antigen specific T-cell activation, Small 11 (13) (2015) 1519–1525.
[20] A.N. Hasan, A. Selvakumar, R.J. O'Reilly, Artificial antigen presenting cells: an off the shelf approach for generation of desirable T-cell populations for broad application of adoptive immunotherapy, Adv. Genet. Eng. 4 (3) (2015).
[21] J. Hendriks, L.A. Gravestein, K. Tesselaar, R.A.W. van Lier, T.N.M. Schumacher, J. Borst, CD27 is required for generation and long-term maintenance of T cell immunity, Nat. Immunol. 1 (5) (2000) 433–440.
[22] R. Zappasodi, C. Sirard, Y.Y. Li, S. Budhu, M. Abu-Akeel, C.L. Liu, X. Yang, H. Zhong, W. Newman, J.J. Qi, P. Wong, D. Schaer, H. Koon, V. Velcheti, M. D. Hellmann, M.A. Postow, M.K. Callahan, J.D. Wolchok, T. Merghoub, Rational design of anti-GITR-based combination immunotherapy, Nat. Med. 25 (5) (2019) 759–+.
[23] A.D. Waldman, J.M. Fritz, M.J. Lenardo, A guide to cancer immunotherapy: from T cell basic science to clinical practice, Nat. Rev. Immunol. 20 (11) (2020) 651–668.
[24] C.M.J. Hu, R.H. Fang, K.C. Wang, B.T. Luk, S. Thamphiwatana, D. Dehaini, P. Nguyen, P. Angsantikul, C.H. Wen, A.V. Kroll, C. Carpenter, M. Ramesh, V. Qu, S.H. Patel, J. Zhu, W. Shi, F.M. Hofman, T.C. Chen, W.W. Gao, K. Zhang, S. Chien, L.F. Zhang, Nanoparticle biointerfacing by platelet membrane cloaking, Nature 526 (7571) (2015) 118–+.
[25] P. Hansrivijit, R.P. Gale, J. Barrett, S.O. Ciurea, Cellular therapy for acute myeloid Leukemia - current status and future prospects, Blood Rev. 37 (2019).
[26] T.C. Ho, H.S. Kim, Y.M. Chen, Y.M. Li, M.W. LaMere, C. Chen, H. Wang, J. Gong, C. D. Palumbo, J.M. Ashton, H. Kim, Q.B. Xu, M.W. Becker, K.W. Leong, Scaffold-mediated CRISPR-Cas9 delivery system for acute myeloid leukemia therapy, Sci. Adv. 7 (21) (2021).
[27] N. Kotagiri, Z. Li, X. Xu, S. Mondal, A. Nehorai, S. Achilefu, Antibody quantum dot conjugates developed via copper-free click chemistry for rapid analysis of biological samples using a microfluidic microsphere array system, Bioconjugate Chem. 25 (7) (2014) 1272–1281.
[28] M. Hommel, B. Kyewski, Dynamic changes during the immune response in T cell-antigen-presenting cell clusters isolated from lymph nodes, J. Exp. Med. 197 (3) (2003) 269–280.

[29] J.W. Hickey, F.P. Vicente, G.P. Howard, H.Q. Mao, J.P. Schneck, Biologically inspired design of nanoparticle artificial antigen-presenting cells for immunomodulation, Nano Lett. 17 (11) (2017) 7045–7054.
[30] M. Aleksic, O. Dushek, H. Zhang, E. Shenderov, J.L. Chen, V. Cerundolo, D. Coombs, P.A. van der Merwe, Dependence of T Cell antigen recognition on T cell receptor-peptide MHC confinement time, Immunity 32 (2) (2010) 163–174.
[31] C. Zhu, N. Jiang, J. Huang, V.I. Zarnitsyna, B.D. Evavold, Insights from in situ analysis of TCR-pMHC recognition: response of an interaction network, Immunol. Rev. 251 (2013) 49–64.
[32] C. Klammt, B.F. Lillemeier, How membrane structures control T cell signaling, Front. Immunol. 3 (2012).
[33] C.J. Hsu, W.T. Hsieh, A. Waldman, F. Clarke, E.S. Huseby, J.K. Burkhardt, T. Baumgart, Ligand mobility modulates immunological synapse formation and T cell activation, PLoS One 7 (2) (2012).
[34] F. Giannoni, J. Barnett, K. Bi, R. Samodal, P. Lanza, P. Marchese, R. Billetta, R. Vita, M.R. Klein, B. Prakken, W.W. Kwok, E. Sercarz, A. Altman, S. Albani, Clustering of T cell Ligands on artificial APC membranes influences T cell activation and protein kinase C theta translocation to the T cell plasma membrane, J. Immunol. 174 (6) (2005) 3204–3211.
[35] J. Deeg, M. Axmann, J. Matic, A. Liapis, D. Depoil, J. Afrose, S. Curado, M. L. Dustin, J.P. Spatz, T cell activation is determined by the number of presented antigens, Nano Lett. 13 (11) (2013) 5619–5626.
[36] P.A. Gonzalez, L.J. Carreno, D. Coombs, J.E. Mora, E. Palmieri, B. Goldstein, S. G. Nathenson, A.M. Kalergis, T cell receptor binding kinetics required for T cell activation depend on the density of cognate ligand on the antigen-presenting cell, P Natl Acad Sci USA 102 (13) (2005) 4824–4829.
[37] W.S. Chen, Q.Z. Zhang, B.T. Luk, R.H. Fang, Y.N. Liu, W.W. Gao, L.F. Zhang, Coating nanofiber scaffolds with beta cell membrane to promote cell proliferation and function, Nanoscale 8 (19) (2016) 10364–10370.
[38] H.S. Kim, N. Mandakhbayar, H.W. Kim, K.W. Leong, H.S. Yoo, Protein-reactive nanofibrils decorated with cartilage-derived decellularized extracellular matrix for osteochondral defects, Biomaterials 269 (2021).
[39] X. Qin, Y. Wu, S. Liu, L. Yang, H. Yuan, S. Cai, J. Flesch, Z. Li, Y. Tang, X. Li, Y. Zhuang, C. You, C. Liu, C. Yu, Surface modification of polycaprolactone scaffold with improved biocompatibility and controlled growth factor release for enhanced stem cell differentiation, Front. Bioeng. Biotechnol. 9 (2021), 802311.
[40] W.J. King, P.H. Krebsbach, Growth factor delivery: how surface interactions modulate release in vitro and in vivo, Adv. Drug Deliv. Rev. 64 (12) (2012) 1239–1256.
[41] V. Luginbuehl, L. Meinel, H.P. Merkle, B. Gander, Localized delivery of growth factors for bone repair, Eur. J. Pharm. Biopharm. 58 (2) (2004) 197–208.
[42] C.A. Sabatos, J. Doh, S. Chakravarti, R.S. Friedman, P.G. Pandurangi, A.J. Tooley, M.F. Krummel, A synaptic basis for paracrine interleukin-2 signaling during homotypic T cell interaction, Immunity 29 (2) (2008) 238–248.
[43] M. Huse, E.J. Quann, M.M. Davis, Shouts, whispers and the kiss of death: directional secretion in T cells, Nat. Immunol. 9 (10) (2008) 1105–1111.
[44] E.R. Steenblock, T. Fadel, M. Labowsky, J.S. Pober, T.M. Fahmy, An artificial antigen-presenting cell with paracrine delivery of IL-2 impacts the magnitude and direction of the T cell response, J. Biol. Chem. 286 (40) (2011) 34883–34892.
[45] S.B. Stephan, A.M. Taber, I. Jileaeva, E.P. Pegues, C.L. Sentman, M.T. Stephan, Biopolymer implants enhance the efficacy of adoptive T-cell therapy, Nat. Biotechnol. 33 (1) (2015) 97–101.
[46] Z. Ren, A. Zhang, Z. Sun, Y. Liang, J. Ye, J. Qiao, B. Li, Y.X. Fu, Selective delivery of low-affinity IL-2 to PD-1+ T cells rejuvenates antitumor immunity with reduced toxicity, J. Clin. Invest. 132 (3) (2022).
[47] E.E. West, H.T. Jin, A.U. Rasheed, P. Penaloza-Macmaster, S.J. Ha, W.G. Tan, B. Youngblood, G.J. Freeman, K.A. Smith, R. Ahmed, PD-L1 blockade synergizes with IL-2 therapy in reinvigorating exhausted T cells, J. Clin. Invest. 123 (6) (2013) 2604–2615.
[48] Y.M. Shin, T.G. Kim, J.S. Park, H.J. Gwon, S.I. Jeong, H. Shin, K.S. Kim, D. Kim, M. H. Yoon, Y.M. Lim, Engineered ECM-like microenvironment with fibrous particles for guiding 3D-encapsulated hMSC behaviours, J. Mater. Chem. B 3 (13) (2015) 2732–2741.
[49] T. Ahmad, J. Lee, Y.M. Shin, H.J. Shin, S.K.M. Perikamana, S.H. Park, S.W. Kim, H. Shin, Hybrid-spheroids incorporating ECM like engineered fragmented fibers potentiate stem cell function by improved cell/cell and cell/ECM interactions, Acta Biomater. 64 (2017) 161–175.
[50] M. Patel, W.G. Koh, Composite hydrogel of methacrylated hyaluronic acid and fragmented polycaprolactone nanofiber for osteogenic differentiation of adipose-derived stem cells, Pharmaceutics 12 (9) (2020).
[51] A.J.R. Amaral, G. Pasparakis, Cell membrane engineering with synthetic materials: applications in cell spheroids, cellular glues and microtissue formation, Acta Biomater. 90 (2019) 21–36.
[52] H.Z. Yan, D. Shao, Y.H. Lao, M.Q. Li, H.Z. Hu, K.W. Leong, Engineering cell membrane-based nanotherapeutics to target inflammation, Adv. Sci. 6 (15) (2019).
[53] H.S. Kim, H.S. Yoo, Surface-polymerized biomimetic nanofibrils for the cell-directed association of 3-D scaffolds, Chem. Commun. 51 (2) (2015) 306–309.